

## LYMPHOID NEOPLASIA

## ABT-199 mediated inhibition of BCL-2 as a novel therapeutic strategy in T-cell acute lymphoblastic leukemia

Sofie Peirs,<sup>1</sup> Filip Matthijssens,<sup>1</sup> Steven Goossens,<sup>2</sup> Inge Van de Walle,<sup>3</sup> Katia Ruggero,<sup>4</sup> Charles E. de Bock,<sup>5</sup> Sandrine Degryse,<sup>5</sup> Kirsten Canté-Barrett,<sup>6</sup> Delphine Briot,<sup>7</sup> Emmanuelle Clappier,<sup>7</sup> Tim Lammens,<sup>8</sup> Barbara De Moerloose,<sup>8</sup> Yves Benoit,<sup>8</sup> Bruce Poppe,<sup>1</sup> Jules P. Meijerink,<sup>6</sup> Jan Cools,<sup>5</sup> Jean Soulier,<sup>7</sup> Terence H. Rabbitts,<sup>4</sup> Tom Taghon,<sup>3</sup> Frank Speleman,<sup>1</sup> and Pieter Van Vlierberghe<sup>1</sup>

<sup>1</sup>Center for Medical Genetics, <sup>2</sup>Flanders Institute for Biotechnology Inflammation Research Center, and <sup>3</sup>Department of Clinical Chemistry, Microbiology and Immunology, Ghent University, Ghent, Belgium; <sup>4</sup>Medical Research Council Molecular Haematology Unit, Weatherall Institute of Molecular Medicine, University of Oxford, John Radcliffe Hospital, Oxford, England, United Kingdom; <sup>5</sup>Laboratory for the Molecular Biology of Leukemia, Center for Human Genetics, University of Leuven and Center for the Biology of Disease, Vlaams Instituut voor Biotechnologie, Leuven, Belgium; <sup>6</sup>Department of Pediatric Oncology/Hematology, Erasmus Medical Center, Rotterdam, The Netherlands; <sup>7</sup>Genome Rearrangements and Cancer Laboratory, U462 INSERM, Laboratoire Central d'Hématologie and Institut Universitaire d'Hématologie, Hôpital Saint-Louis, Paris, France; and <sup>8</sup>Department of Pediatric Hematology-Oncology and Stem Cell Transplantation, Ghent University Hospital, Ghent, Belgium

## Key Points

- High levels of the anti-apoptotic factor BCL-2 can be therapeutically exploited by the BH3 mimetic ABT-199 in human T-ALL.

T-cell acute lymphoblastic leukemia (T-ALL) is a high-risk subtype of acute lymphoblastic leukemia (ALL) with gradually improved survival through introduction of intensified chemotherapy. However, therapy-resistant or refractory T-ALL remains a major clinical challenge. Here, we evaluated B-cell lymphoma (BCL)-2 inhibition by the BH3 mimetic ABT-199 as a new therapeutic strategy in human T-ALL. The T-ALL cell line LOUCY, which shows a transcriptional program related to immature T-ALL, exhibited high *in vitro* and *in vivo* sensitivity for ABT-199 in correspondence with high levels of BCL-2. In addition, ABT-199 showed synergistic therapeutic effects with different chemotherapeutic agents

including doxorubicin, L-asparaginase, and dexamethasone. Furthermore, *in vitro* analysis of primary patient samples indicated that some immature, *TLX3*- or *HOXA*-positive primary T-ALLs are highly sensitive to BCL-2 inhibition, whereas *TAL1* driven tumors mostly showed poor ABT-199 responses. Because *BCL-2* shows high expression in early T-cell precursors and gradually decreases during normal T-cell differentiation, differences in ABT-199 sensitivity could partially be mediated by distinct stages of differentiation arrest between different molecular genetic subtypes of human T-ALL. In conclusion, our study highlights BCL-2 as an attractive molecular target in specific subtypes of human T-ALL that could be exploited by ABT-199. (*Blood*. 2014;124(25):3738-3747)

## Introduction

T-cell acute lymphoblastic leukemia (T-ALL) is an aggressive hematologic cancer that occurs in children and adolescents. Despite significant insights in T-ALL biology, only limited therapeutic options are available for patients with primary resistant or relapsed disease. Current T-ALL treatment schedules consist of high-dose chemotherapy and are often associated with acute and chronic life-threatening and debilitating toxicities.<sup>1-3</sup> Consequently, there is an urgent clinical need for optimized treatment stratification and more effective antileukemic drugs for the treatment of human T-ALL.<sup>3</sup>

Genetic studies have collectively shown that T-ALLs can be divided into subgroups that are characterized by unique gene expression signatures and relate to stages of T-cell differentiation at which the leukemic cells arrest. Each molecular subgroup has characteristic genetic abnormalities that cause aberrant activation of specific T-ALL transcription factor oncogenes, including *LYL1/MEF2C*, *HOXA*, *TLX1*, *TLX3*, and *TAL1/LMO2* driven T-ALL.<sup>3-6</sup> Notably, the recently described early T-cell precursor (ETP)-acute lymphoblastic leukemia (ALL) patients<sup>7</sup> have leukemic cells that show an

early block in T-cell differentiation and significantly overlap with *LYL1*-positive T-ALL<sup>4</sup> and *MEF2C*-dysregulated immature T-ALL.<sup>5,8</sup> These immature T-cell leukemias often express myeloid markers such as CD13 and CD33, and show a transcriptional program related to hematopoietic stem cells and myeloid progenitors.<sup>5</sup> Importantly, these tumors are associated with poor prognosis and reduced overall survival.<sup>7,9,10</sup> Preclinical mouse models of *LMO2*-dependent T-cell neoplasia are thought to recapitulate at least some features of early immature human T-ALL including a pre-leukemic T-cell differentiation arrest.<sup>11</sup> In general, T-ALLs can be classified in pro-T (CD7<sup>+</sup>, CD2<sup>-</sup>, CD5<sup>-</sup>), pre-T (CD7<sup>+</sup>, CD2<sup>+</sup>, CD5<sup>±</sup>), cortical-T (CD1a<sup>+</sup>), and mature T-cell stages (sCD3<sup>+</sup>, CD1a<sup>-</sup>), according to the European Group for the Immunological Characterization of Leukaemias classification system.<sup>12</sup>

In an effort to improve patient prognosis and survival, targeted therapeutics are beginning to emerge as powerful agents against hematologic malignancies. One such example is the small molecule ABT-199, a highly potent, orally bioavailable B-cell lymphoma

Submitted May 8, 2014; accepted September 25, 2014. Prepublished online as *Blood* First Edition paper, October 9, 2014; DOI 10.1182/blood-2014-05-574566.

The online version of this article contains a data supplement.

The publication costs of this article were defrayed in part by page charge payment. Therefore, and solely to indicate this fact, this article is hereby marked "advertisement" in accordance with 18 USC section 1734.

© 2014 by The American Society of Hematology

(BCL)-2 specific inhibitor.<sup>13</sup> The anti-tumor effects of ABT-199 have been reported in a growing number of tumor entities, including acute myeloid leukemia,<sup>14,15</sup> chronic lymphocytic leukemia (CLL),<sup>16</sup> multiple myeloma,<sup>17</sup> estrogen receptor-positive breast cancer,<sup>18</sup> and lymphoma.<sup>19</sup> Currently, phase-I clinical trials of ABT-199 in CLL are ongoing and the first preliminary results show a high overall response rate. Notably, some patients included in this trial experienced tumor lysis syndrome as a result of the massive cell death induced by ABT-199.<sup>20</sup>

Given these promising antitumor results for ABT-199, we sought to establish the extent and level of BCL-2 expression across different T-ALL molecular subgroups and evaluated the therapeutic potential of the BCL-2 inhibitor ABT-199 in the context of human T-ALL.

## Methods

### Patient samples, cell lines, and mouse tumor cells

The cell lines were purchased from the DSMZ repository (Braunschweig, Germany) and cultured in RPMI 1640 medium supplemented with 10% or 20% fetal bovine serum (FBS), 100 U/mL penicillin, 100 µg/mL streptomycin, 100 µg/mL kanamycin sulfate, and 2 mM L-glutamine at 37°C with 5% CO<sub>2</sub>.

Bone marrow lymphoblast samples from 64 T-ALL patients (15 immature, 25 *TAL/LMO*, 17 *TLX1/TLX3*, and 7 *HOXA*) were collected with informed consent, according to the declaration of Helsinki from Saint-Louis Hospital, Paris, France, and the study was approved by the Institut Universitaire d'Hématologie Institutional Review Board. This primary T-ALL cohort was previously investigated<sup>21</sup> and the high-quality RNA samples from this cohort were used for gene expression profiling.

Primary T-ALL cells for in vitro ABT-199 treatment and xenograft studies were acquired by informed consent from the Department of Pediatric Hemato-Oncology at Ghent University Hospital. These primary T-ALL samples were assigned to a specific molecular genetic subclass based on real-time polymerase chain reaction (RT-PCR) of *SIL-TALI*, or *MLL* fusion transcripts, *TLX1/TLX3* expression analysis by quantitative polymerase chain reaction, or fluorescence in situ hybridization analysis of the *LMO2* locus.

Leukemic T-cells obtained from splenic tissue derived from secondary transplanted tumors that originally developed in the Lck-Lmo2 mouse model (K.R. and T.H.R., manuscript in preparation) were a kind gift of T.H.R.

### Isolation of thymocyte subsets from human thymus tissue

Human thymocytes were extracted from thymus tissue from children undergoing cardiac surgery and were obtained and used according to the guidelines of the Medical Ethical Commission of the Ghent University Hospital, Belgium. The thymus was dissected into small pieces and the released cell suspension was passed through a 40 µm cell strainer. Enrichment of viable mononuclear cells was done by a Lymphoprep density gradient.

CD34-positive cells were isolated by magnetic activated cell sorting (MACS) and purified by fluorescence-activated cell sorter (FACS)-mediated cell sorting. For the isolation of immature single positive cells (CD4<sup>+</sup>CD8<sup>-</sup>CD3<sup>-</sup>), the cells were first labeled with an unlabeled anti-glycophorin-A monoclonal antibody, and subsequently with unlabeled anti-CD8 and anti-CD3 monoclonal antibodies for depletion of residual red blood cells and CD8<sup>+</sup> and CD3<sup>+</sup> cells. Magnetic anti-mouse immunoglobulin-coated Dynabeads were used to obtain a CD3, CD8, and red blood cell depleted thymocyte fraction by means of the DynaMag magnet. This fraction could then be further purified into pre- and post-β-selection CD4<sup>+</sup>CD3<sup>-</sup>CD8<sup>-</sup>CD28<sup>-</sup>, and CD4<sup>+</sup>CD3<sup>-</sup>CD8<sup>-</sup>CD28<sup>+</sup> subsets by staining the cells with anti-human CD4, CD3, CD34, CD8, and CD28 antibodies followed by FACS. Isolation of double-positive and single-positive thymocytes was performed by staining the cells with CD4, CD8, and CD3 antibodies followed by FACS analysis. T-cell receptor (TCR)γδ<sup>+</sup> cells were isolated via MACS by labeling the thymocytes with anti-TCRγδ Hapten antibodies and adding MACS Anti-Hapten MicroBeads fluorescein isothiocyanate. To separate immature and mature TCRγδ<sup>+</sup> cells, the MACS-enriched cells were stained with CD3 and CD1 monoclonal antibodies and sorted via FACS.

### Gene expression profiling of primary T-ALL samples and T-cell subsets

Total RNA was isolated using the miRNeasy mini kit (Qiagen) and the RNA quality was evaluated on the Agilent 2100 bioanalyzer (Agilent Technologies, Santa Clara, CA). Whole human genome expression profiling was performed using the GeneChip Human Genome U133 2.0 Plus arrays (Affymetrix, Santa Clara, CA), according to standardized procedures at the IGBMC (www.igbmc.fr; Strasbourg, France). Normalization of microarray intensities was done using the variance stabilization and calibration (VSN) R package in R. Differential expression analysis was done using the Comparative Marker Selection module in GenePattern.<sup>22</sup> Microarray data have been deposited in the GEO with accession number GSE62156.

### Treatment of cells with ABT-199 followed by viability or apoptosis assay

Cells from T-ALL cell lines (supplemental Table 1, available on the *Blood* Web site) were plated at 100 000 cells per well in 96-well plates. The cells were incubated for 48 hours in 100 µL medium with 10% FBS to which 5 µL of the appropriate ABT-199 dilution or dimethylsulfoxide (DMSO) was added. The assays were performed with the Celltiter-Glo Luminescent Cell Viability Assay according to the manufacturer's instructions (Promega). To determine the half maximal inhibitory concentration (IC<sub>50</sub>), 6 to 8 concentration points (twofold increase) were chosen for each cell line so that the IC<sub>50</sub> point was approximately in the middle of the concentration range. The IC<sub>50</sub> values were calculated using the CalcuSyn software (Biosoft, Cambridge, MA). The experiment was performed 2 or 3 times independently and in every experiment, each concentration was tested in duplicate for every cell line.

For the apoptosis assay, cells were plated at 10 000 cells per well in 96-well plates. The cells were incubated for 24 hours in 95 µL medium with 10% FBS to which 5 µL of the appropriate ABT-199 dilution or DMSO was added. The assay was performed with the Caspase-Glo 3/7 Assay according to the manufacturer's instructions (Promega). The experiment was performed 3 times and every concentration point was each time tested in duplicate for each cell line.

For the treatment of primary T-ALLs, enriched mononuclear cells or full bone marrow from primary leukemia samples were suspended in complete culture medium supplemented with 10% FBS. Cells were plated at 50 000 cells per well in 96-well plates to which 5 µL of the appropriate ABT-199 dilution (9 to 13 concentrations) or DMSO was added (total volume 100 µL). Cell viability was measured 16 hours after adding the compound and the IC<sub>50</sub> values were calculated. Each concentration was tested in duplicate for every patient sample. The Lck-Lmo2 mouse tumor T-cells were thawed and treated with ABT-199 in medium with 10% FBS for 16 hours. The IC<sub>50</sub> values were determined as described above (50 000 cells per well). Two independent experiments were performed in which each concentration was tested in duplicate.

### The quantitative real-time polymerase chain reactions

Total RNA was isolated using the miRNeasy mini kit (Qiagen) and the RNase-Free Dnase set (Qiagen). The iScript cDNA synthesis kit (Bio-Rad) was used to synthesize cDNA. The quantitative real-time polymerase chain reactions were performed using the SsoAdvanced SYBR Green Supermix (Bio-Rad) and were run on the LightCycler 480 (Roche, model LC480). Every sample was analyzed in duplicate and the gene expression was standardized against at least 3 housekeeping genes. The primer sequences are listed in supplemental Table 2.

### Western blotting

Cells were lysed with radioimmunoprecipitation assay (RIPA) buffer and protein concentration was measured with the Pierce BCA protein assay kit. Denatured protein was loaded on a 10% polyacrylamide gel and the sodium dodecyl sulfate-polyacrylamide gel electrophoresis was run followed by western blotting on a nitrocellulose membrane. The primary antibodies used were: Bcl-2 antibody (C-2) (sc-7382; Santa Cruz Biotechnology; dilution 1:1000), BCL-X<sub>L</sub> antibody (#2762; Cell Signaling Technology; dilution 1:1000), and anti-β-actin antibody (Clone AC-75; A2228; Sigma-Aldrich; dilution 1:2000). The protein bands were densitometric analyzed using ImageJ software (National Institutes of Health).

### In vivo treatment of xenografts with ABT-199

Luciferase-positive LOUCY cells were generated by infecting the LOUCY cell line with WPPI-LUC lentiviruses. Nonconcentrated virus was produced in HEK293TN cells using JetPEI polyplus reagent with pMD2.G (envelope plasmid), pSPAX2 (packaging plasmid), and pWPPI-LUC (target plasmid) in 0.1/0.9/1 ratios. Transduced cells expressing enhanced green fluorescent protein were selected 72 hours after infection by cell sorting on a S3 cell sorter (Bio-Rad).

Nonobese diabetic/severe combined immunodeficient  $\gamma$  (NSG) mice were injected at 6 weeks of age in the tail vein with 150  $\mu$ L phosphate-buffered saline containing  $5 \times 10^6$  luciferase-labeled LOUCY cells. At regular time points, the bioluminescence was measured using the IVIS Lumina II imaging system (PerkinElmer). At 6 weeks, the cells were engrafted and the mice were randomly divided into 2 groups (with an equal number of males and females in both groups), and the treatment was started on day 0. Mice were treated with 100 mg ABT-199/kg body weight or with vehicle via oral gavage for 4 consecutive days. ABT-199 was formulated in 60% phosal 50 propylene glycol, 30% polyethylene glycol 400, and 10% ethanol. At days 0, 2, and 4 the bioluminescence was measured. Before imaging, the mice were injected intraperitoneally with 200  $\mu$ L of a 15 mg/mL firefly D-luciferin potassium salt solution and anesthetized by inhalation of 5% isoflurane. The mice were imaged 10 minutes after luciferin injection. The total bioluminescence signal in each mouse was calculated via the region of interest tool (total counts) in the Living Image software (PerkinElmer).

A xenograft of primary human T-ALL cells from patient 3 was established in NSG mice by retro-orbital injection.<sup>21</sup> Upon establishment of disease, human leukemic cells were isolated from the spleen and retransplanted into secondary recipients. Next, tertiary xenograft injections were performed in a cohort of 10 NSG mice and leukemia engraftment was monitored by human CD45 staining (CD45-FITC antibody; Miltenyi Biotec) in peripheral blood using FACS analysis with the S3 cell sorter (Bio-Rad). Upon detection of human CD45<sup>+</sup> leukemic blasts in peripheral blood, mice were randomized in 2 groups and treated with vehicle or 100 mg ABT-199/kg body weight for 7 consecutive days. After treatment, animals were sacrificed and the percentage human CD45-positive leukemic blasts in bone marrow were determined by FACS as described above.

The ethical committee on animal welfare at Ghent University Hospital approved all animal experiments.

### Combination treatment of cells with ABT-199 and chemotherapeutic agents

T-ALL cell lines were plated at 20 000 cells per well in 96-well plates, and twofold dilution series of ABT-199 and the chemotherapeutic were made around the IC<sub>50</sub> point for every cell line. For the combination therapy, 5  $\mu$ L of each compound dilution was added at a constant concentration ratio and every concentration point was tested in duplicate within 1 experiment. The final concentration of solvent was equal for all the concentrations of a particular compound. Cell viability was assessed 48 hours after adding the compounds by CellTiter-Glo Assay, and CalcuSyn was used to calculate the combination index. The chemotherapeutics used were: doxorubicin hydrochloride (D1515, solvent dimethylsulfoxide; Sigma-Aldrich), L-asparaginase (Erwinase, PL 01511/0272, solvent NaCl 0.9%), and dexamethasone (Acadexam; NV Organon; solvent water).

### Statistical analysis

GraphPad Prism 5.04 (La Jolla, CA) was used for statistical analyses.

## Results

### BCL-2 expression in genetic subtypes of human T-ALL and normal T-cells

To evaluate BCL-2 as a potential therapeutic target in human T-ALL, we analyzed BCL-2 expression levels in T-ALL patients and sorted

subsets of normal human thymocytes. Here, we performed microarray gene expression profiling on a panel of 64 primary T-ALL samples and used these gene expression signatures to define different molecular-genetic subtypes of human T-ALL as previously described.<sup>6</sup> Notably, this analysis revealed that high expression of antiapoptotic BCL-2 is a hallmark of immature subtypes of T-ALL (Figure 1A). Moreover, BCL-2 levels were variable in *TLX1*, *TLX3*, and *HOXA* driven T-ALLs and predominantly low in *TAL1* rearranged T-cell leukemias (Figure 1A). Importantly, these findings were validated and confirmed in an independent cohort of 117 genetically well-characterized human T-ALL samples for which gene expression signatures are publically available<sup>5</sup> (Figure 1B). In this validation series, the average BCL-2 expression in the *HOXA* subgroup was similar to the one in the immature T-ALL subgroup.

As normal T-cell development serves as the conceptual framework for the understanding of T-ALL biology,<sup>23</sup> we hypothesized that high BCL-2 expression in immature T-ALL is a reflection of the spatiotemporal regulation of BCL-2 during normal T-cell development. Indeed, BCL-2 expression was high in CD34<sup>+</sup> T-cell progenitors and gradually decreased during differentiation with the lowest values in CD4<sup>+</sup>CD8<sup>+</sup> double-positive T-cells (supplemental Figure 1A). Interestingly, BCL-2L1 (the gene encoding BCL-X<sub>L</sub>) expression showed an inverse trend (supplemental Figure 1A). Furthermore, BCL-2 and BCL-X<sub>L</sub> expression in CD34<sup>+</sup> T-cell progenitors as compared with sorted CD4<sup>+</sup>CD8<sup>+</sup> and TCR $\gamma\delta$ <sup>+</sup> T-cell fractions was confirmed at the protein level (supplemental Figure 1B).

### ABT-199 sensitivity in human T-ALL cell lines

Next, we determined IC<sub>50</sub> values for ABT-199 in a panel of 11 human T-ALL cell lines. Mature T-ALL cell lines, including ALL-SIL, CUTLL1, TALL-1, KOPTK1, DND-41, PF-382, KARPAS-45, PEER, JURKAT, and CCRF-CEM showed modest responses toward ABT-199 treatment with IC<sub>50</sub> values ranging from 0.2 to 10  $\mu$ M (Figure 2A). Most notably and in-line with a previous report,<sup>24</sup> the T-ALL cell line LOUCY, which shows a transcriptional program related to early immature T-ALLs,<sup>25</sup> was highly sensitive toward ABT-199 treatment (IC<sub>50</sub> = 13.9 nM). As expected, induction of apoptosis upon treatment of LOUCY with 20 nM ABT-199 for 24 hours was associated with increased caspase activity (Figure 2B). This induction at low ABT-199 concentration was significantly higher ( $P = .0088$ ; 2-sided  $t$  test) in LOUCY cells as compared with ALL-SIL, the second most ABT-199 sensitive T-ALL cell line (Figure 2B). Moreover, we observed a negative correlation between ABT-199 IC<sub>50</sub> values and BCL-2 messenger RNA (Spearman  $\rho = -0.855$ ;  $P = .0015$ ) and BCL-2 protein (Spearman  $\rho = -0.7$ ;  $P = .0204$ ) levels in human T-ALL cell lines (Figure 2C-F).

To test the efficacy of ABT-199 in vivo, we performed xenograft experiments using luciferase positive LOUCY cells in immunodeficient NSG mice (Figure 3). Treatment of established xenografted tumors with 100 mg ABT-199/kg for 4 days resulted in a significant reduction of leukemic burden ( $P = .0048$ ; 2-sided  $t$  test), suggesting that BCL-2 inhibition can selectively restrain leukemic cell growth of the T-ALL cell line LOUCY in vivo.

### Mouse model of immature T-ALL responds to ABT-199

To further study the association between ABT-199 sensitivity and tumor immune phenotype in T-ALL, we used the Lck-Lmo2 transgenic mouse model. Overexpression of the *Lmo2* oncogene in the thymi of these Lck-Lmo2 mice results in the development of murine T-cell tumors with an average latency of 10 months (K.R. and T.H.R., manuscript in preparation), comparable to the CD2-Lmo2 transgenic

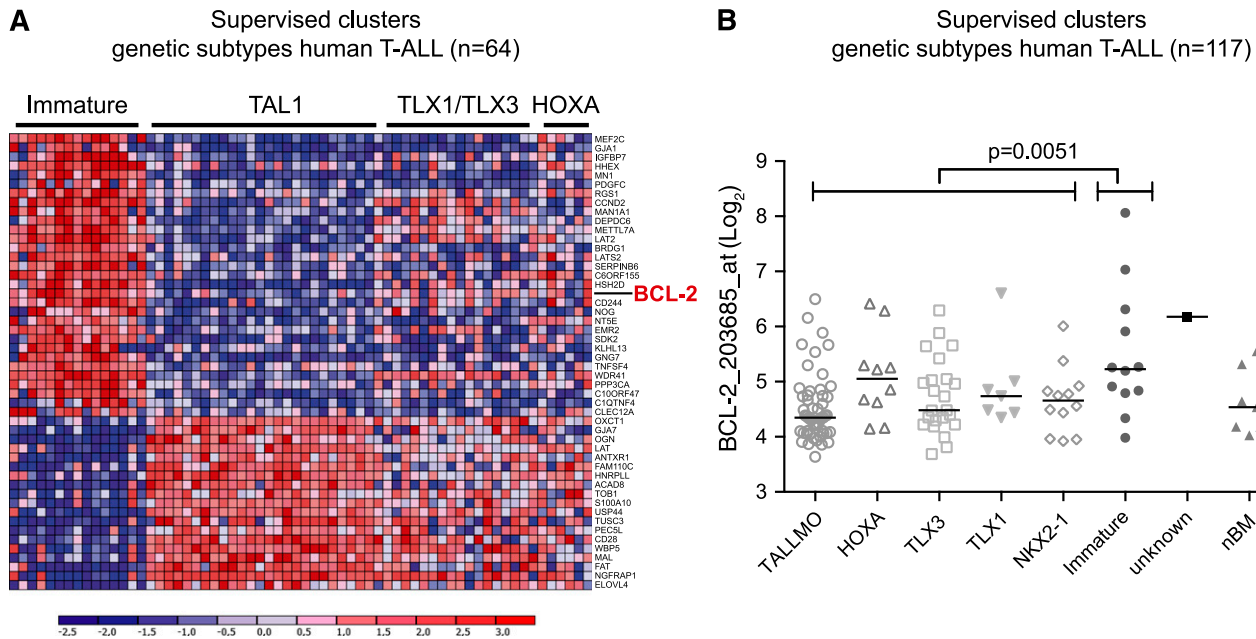


**Figure 1. *BCL-2* expression in malignant human T-cells.** (A) Differential gene expression profiling of primary immature T-ALLs vs T-ALLs from other subgroups ( $\log_2[\text{fold change}] > 2$ ;  $P < .05$ ). A heat map of the top 50 differentially expressed genes is shown. Genes in the heat map are shown in rows and each individual leukemia sample is shown in 1 column. Expression levels are visualized as color-coded differential expression from the mean in standard deviation units with red indicating higher levels and blue lower levels of expression. This primary T-ALL cohort has previously been investigated<sup>21</sup> and hierarchical clustering was used to define molecular-genetic subtypes of human T-ALL, as previously described.<sup>6</sup> (B) *BCL-2* expression levels (probe 203685\_at) in an independent cohort of 117 human T-ALL samples. Molecular-genetic subtypes of human T-ALL have been defined as previously described.<sup>5</sup> nBM, normal bone marrow.  $P = 0.0051$ .

strain.<sup>11,26</sup> Interestingly, the resulting Lck-Lmo2 driven murine tumors show considerable immunophenotypic tumor heterogeneity, providing an opportunity to study the potential connection between tumor immunophenotype and ABT-199 response in a homogeneous genetic background.

For this, we determined ABT-199  $IC_{50}$  values in leukemic blasts obtained from 2 immunophenotypically different Lck-Lmo2 murine tumors that sustained their phenotype during transplantation. One Lck-Lmo2 tumor (#39365) showed an immature phenotype with about 90% CD4/CD8 double-negative blasts, whereas the second tumor (#39354) presented with a more mature phenotype consisting of approximately 30% CD4/CD8 double-positive and 40% CD4 single-positive leukemic blasts. Interestingly, we identified a 100-fold difference in ABT-199  $IC_{50}$  value between the immature (#39365;  $IC_{50} = 2.2$  nM) (Figure 4A) and mature murine T-cell tumor (#39354;  $IC_{50} = 214$  nM) (Figure 4A), and this differential ABT-199 response was associated with enhanced levels of *BCL-2* in the immature murine T-cell tumor (Figure 4B).

#### ABT-199 response in primary T-ALL samples

To define ABT-199 sensitivity in primary patient material, we subsequently selected a panel of 17 pediatric primary T-ALL samples that represent major immunophenotypic maturation stages and molecular genetic subtypes of T-ALL (Figure 5A; supplemental Figure 2). Leukemic samples belonging to the early stages of maturation based on the European Group for the Immunological Characterization of Leukaemias criteria<sup>12</sup> were predominantly sensitive to ABT-199 treatment with all CD4<sup>-</sup> CD8<sup>-</sup> double negative T-ALL samples showing an  $IC_{50}$  lower than 300 nM. In contrast, mature T-ALL patient samples showed modest ABT-199 responses with the most SIL-TAL1-positive T-ALLs showing an  $IC_{50} > 800$  nM. Although only few *HOXA* and *TLX3* rearranged T-ALLs were included in this patient series, some *TLX3*- or *HOXA*-positive

leukemias were also highly sensitive to *BCL-2* inhibition (Figure 5A; supplemental Figure 2).

Interestingly, the putative relation between tumor immunophenotype and ABT-199 sensitivity was further strengthened by a unique T-ALL sample that presented with a mature T-ALL at diagnosis, but suffered from an immature/biphenotypic T-ALL at relapse 11 months after initial diagnosis (supplemental Figure 3). Notably, the leukemic clone with an immature/biphenotypic immunophenotype that eventually gave rise to the relapse was already detected at day 15 and day 35 after induction therapy. Notably, in vitro analysis of these paired samples obtained at diagnosis and relapse revealed marked differences in ABT-199 sensitivity. The immature leukemic cells at relapse were highly sensitive to ABT-199 treatment ( $IC_{50} = 7.32$  nM), whereas the mature leukemic cell population at diagnosis barely responded to ABT-199 ( $IC_{50} > 800$  nM) (Figure 5B). Interestingly, the marked difference in ABT-199 sensitivity was accompanied by a notable difference in *BCL-2* expression between the diagnostic and relapse sample (Figure 5C).

Finally, we established a patient-derived xenograft in NSG mice from the *HOXA*-positive (*MLL* rearranged) T-ALL patient sample #3 that showed ABT-199 sensitivity in vitro (Figure 5A; supplemental Figure 2). ABT-199 treatment of this patient-derived xenograft for 7 consecutive days resulted in a significant lower percentage of human CD45-positive cells in the bone marrow ( $P = .0498$ ; one-sided *t* test with Welch's correction) as compared with the vehicle-treated mice (Figure 5D).

#### Combination of ABT-199 and chemotherapeutics

To evaluate potential synergism between ABT-199 and conventional chemotherapeutic agents, T-ALL cell lines were treated with combinations of ABT-199 and doxorubicin, L-asparaginase (Erwinase) or dexamethasone (Acidexam). LOUCY and ALL-SIL displayed higher synergism with doxorubicin and L-asparaginase as compared

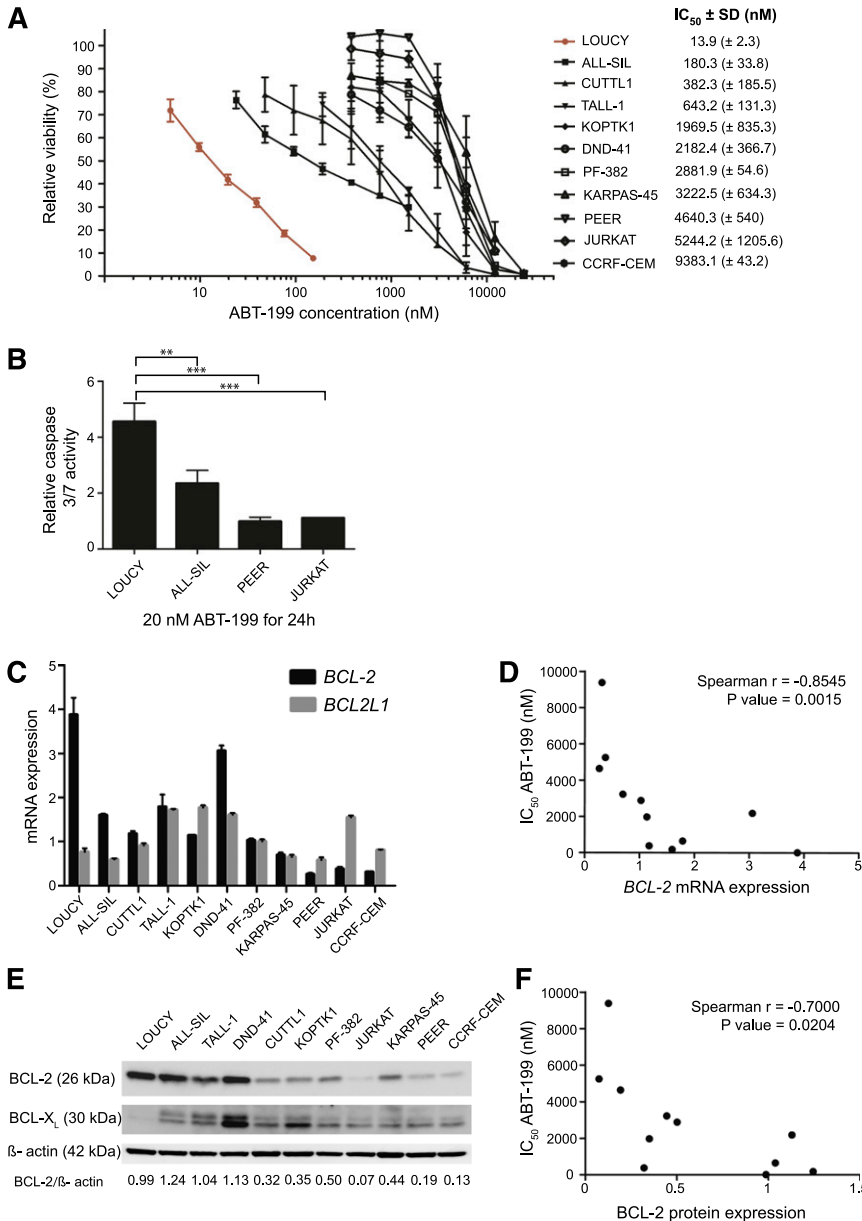


**Figure 2. ABT-199 response in human T-ALL cell lines.** (A) The effect of 48 hours of ABT-199 treatment on the viability of human T-ALL cell lines relative to cells treated with dimethylsulfoxide (100%). The results represent the average and standard deviation for at least 2 independent experiments. SD, standard deviation. (B) Caspase 3/7 activity was measured 24 hours after adding ABT-199 and was plotted relative to the DMSO control. The average and standard deviation of 3 independent experiments is shown. The caspase activity after treatment with 20 nM of ABT-199 was significantly higher in LOUCY than ALL-SIL ( $P = .0088$ ; 2-sided  $t$  test), PEER ( $P = .0008$ ; 2-sided  $t$  test), or JURKAT ( $P = .0119$ ; 2-sided  $t$  test with Welch's correction). (C) *BCL-2* and *BCL-2L1* expression measured with quantitative real-time polymerase chain reactions in a panel of T-ALL cell lines. The graph shows the calibrated normalized relative quantities values and corresponding standard error as calculated with qBasePLUS. The gene expression was standardized against *HMBS*, *TBP*, and *UBC*. (D) Correlation between the IC<sub>50</sub> values for ABT-199 and *BCL-2* mRNA expression in human T-ALL cell lines. (E) Western blot of *BCL-2* and *BCL-XL* in T-ALL cell lines with β-actin as the loading control. (F) Correlation between the IC<sub>50</sub> values for ABT-199 and *BCL-2* protein levels in human T-ALL cell lines.

with the ABT-199-insensitive JURKAT cell line (Figure 6A-B; supplemental Table 3). In addition, the combination of ABT-199 with dexamethasone was strongly synergistic in LOUCY cells (Figure 6C; supplemental Table 3) and was not evaluated in JURKAT and ALL-SIL because of the high dexamethasone IC<sub>50</sub> values in these cell lines.

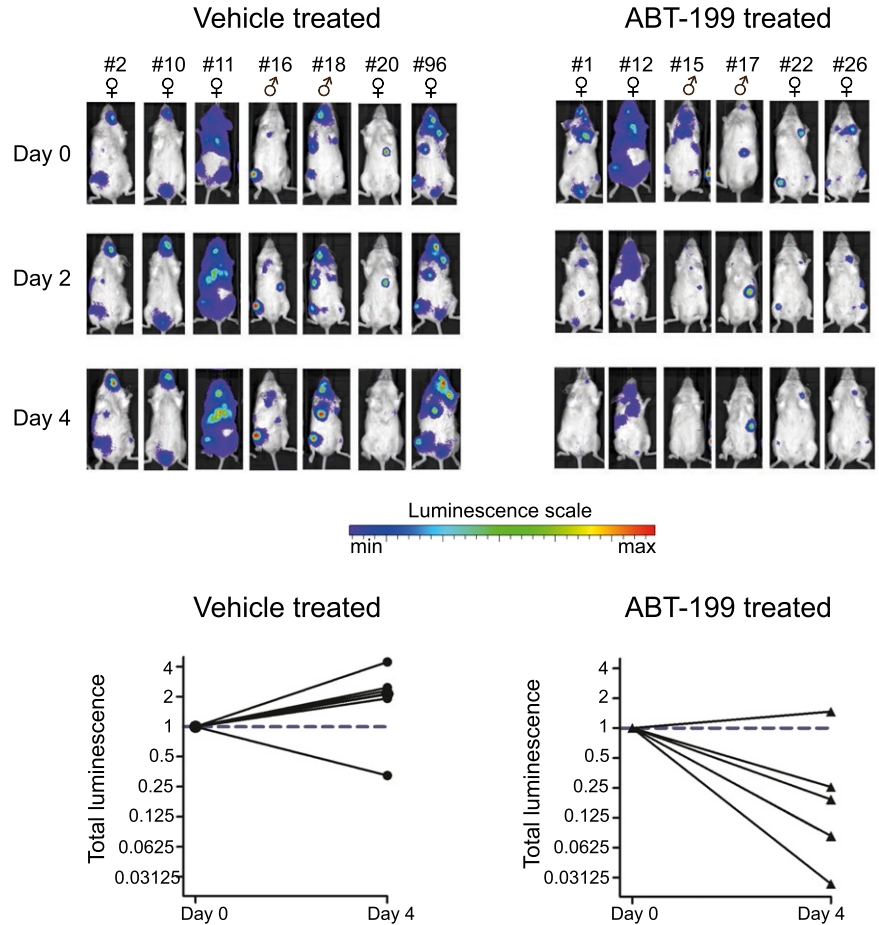
## Discussion

T-ALL is a genetically heterogeneous disease with cure rates in modern protocols reaching >80% in children and approximately 50% in adults.<sup>27</sup> The standard antileukemic therapy consists of intensive multiagent chemotherapy and is associated with considerable toxicities and long-term side effects. Therefore, novel molecularly driven therapeutic approaches should be developed to improve clinical care for T-ALL patients in the near future.

Evasion of apoptosis is a hallmark of human cancer<sup>28</sup> and is often mediated by overexpression of prosurvival BCL-2 family proteins, and can act as a major determinant of chemotherapy resistance.<sup>29</sup> Hence, the search for compounds that could target prosurvival BCL-2 family members has been actively explored.<sup>30</sup> ABT-737<sup>31</sup> and its orally bioavailable derivative ABT-263<sup>32</sup> (navitoclax) are BH3 mimetics that inhibit the antiapoptotic proteins BCL-2, BCL-X<sub>L</sub>, and BCL-W. Initial clinical trials using navitoclax have shown promising antitumoral effects particularly in CLL.<sup>33</sup> Unfortunately, navitoclax treatment was associated with dose-limiting thrombocytopenia, given the critical role of BCL-X<sub>L</sub> in platelet survival.<sup>32,34</sup> As a consequence, ABT-199<sup>13</sup> was developed as a highly specific inhibitor that only targeted BCL-2 and therefore spared platelets.

To evaluate BCL-2 as a molecular target for therapy in human T-ALL, we analyzed the pattern of *BCL-2* expression across 181 primary T-ALL samples and documented high *BCL-2* expression in immature T-ALLs. Notably, these results are in line with a study by Ferrando et al<sup>4</sup> that reported high *BCL-2* expression in so-called *LYL1*

**Figure 3. ABT-199 sensitivity in a mouse xenograft model of the T-ALL cell line LOUCY.** Thirteen mice xenografted with luciferase positive LOUCY cells were vehicle treated or ABT-199 treated (100 mg/kg body weight) for 4 days. The bioluminescence was measured before the start of the treatment (day 0) and after 2 and 4 days of treatment. Each column with pictures represents 1 individual mouse. The total bioluminescence signal after 4 days of treatment is plotted relative to the start value at day 0 for each mouse.



positive T-ALLs, a molecular subtype of human T-ALL that closely resembles immature T-ALL<sup>5</sup> and partially overlaps with the more recently identified subclass of poor prognostic ETP-ALL. In addition, we observed intermediate *BCL-2* expression in *TLX1*, *TLX3*, or *HOXA* driven T-ALLs, whereas mature T-ALLs, which are often characterized by *TAL1* or *Lmo2* oncogene activation, displayed low levels of *BCL-2*.

In the past, transcriptional profiling studies have established a genetic classification of human T-ALL.<sup>4-7</sup> Collectively, these analyses showed

that gene expression signatures of molecular genetic T-ALL subgroups are closely related to those of normal thymocytes at distinct stages of T-cell development.<sup>4</sup> Given this, we analyzed *BCL-2* expression in 11 subsets of human thymocytes that collectively reflect the chronological steps in human T-cell differentiation. Early T-cell precursors that enter the thymus from the bone marrow showed high *BCL-2* levels and this expression pattern was maintained until the CD28<sup>-</sup>CD4<sup>+</sup> immature single positive (ISP) stage. At this point, CD28<sup>-</sup>CD4<sup>+</sup> ISP

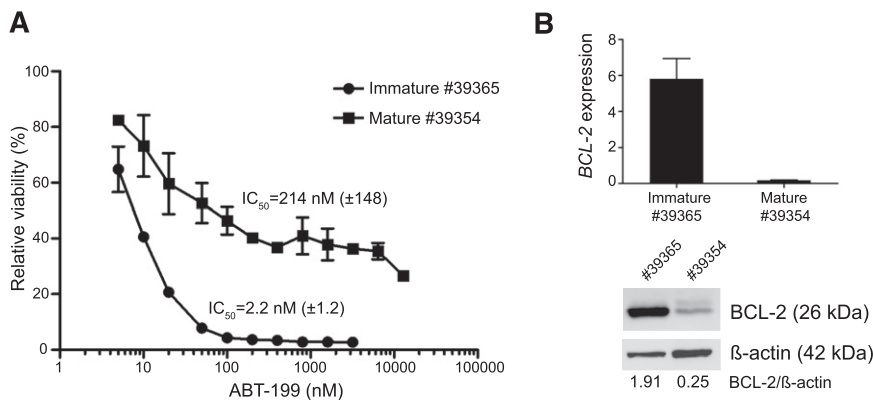


**Figure 4. BCL-2 expression and ABT-199 sensitivity in the Lck-Lmo2 transgenic mouse model.** (A) ABT-199 response of tumor cells obtained from Lck-Lmo2 transgenic mice. T-cell tumor #39365 consists of approximately 90% double-negative T-cells (approximately 40% double-negative 1, 60% double-negative 2), whereas tumor #39354 consists of about 30% double-positive and 40% CD4<sup>+</sup> single-positive T-cells. The viability (average and standard deviation of 2 independent experiments) is shown relative to the cells incubated with dimethylsulfoxide (100%). Based on these data, the IC<sub>50</sub> values were calculated. (B) BCL-2 expression in the Lck-Lmo2 mouse tumors. The top panel shows the mRNA expression (quantitative real-time polymerase chain reactions, calibrated normalized relative quantities values and corresponding standard errors) and the bottom panel shows the protein expression with β-actin as loading control. The messenger RNA gene expression was standardized against *Hmbs*, *Tbp*, and *Ubc*.

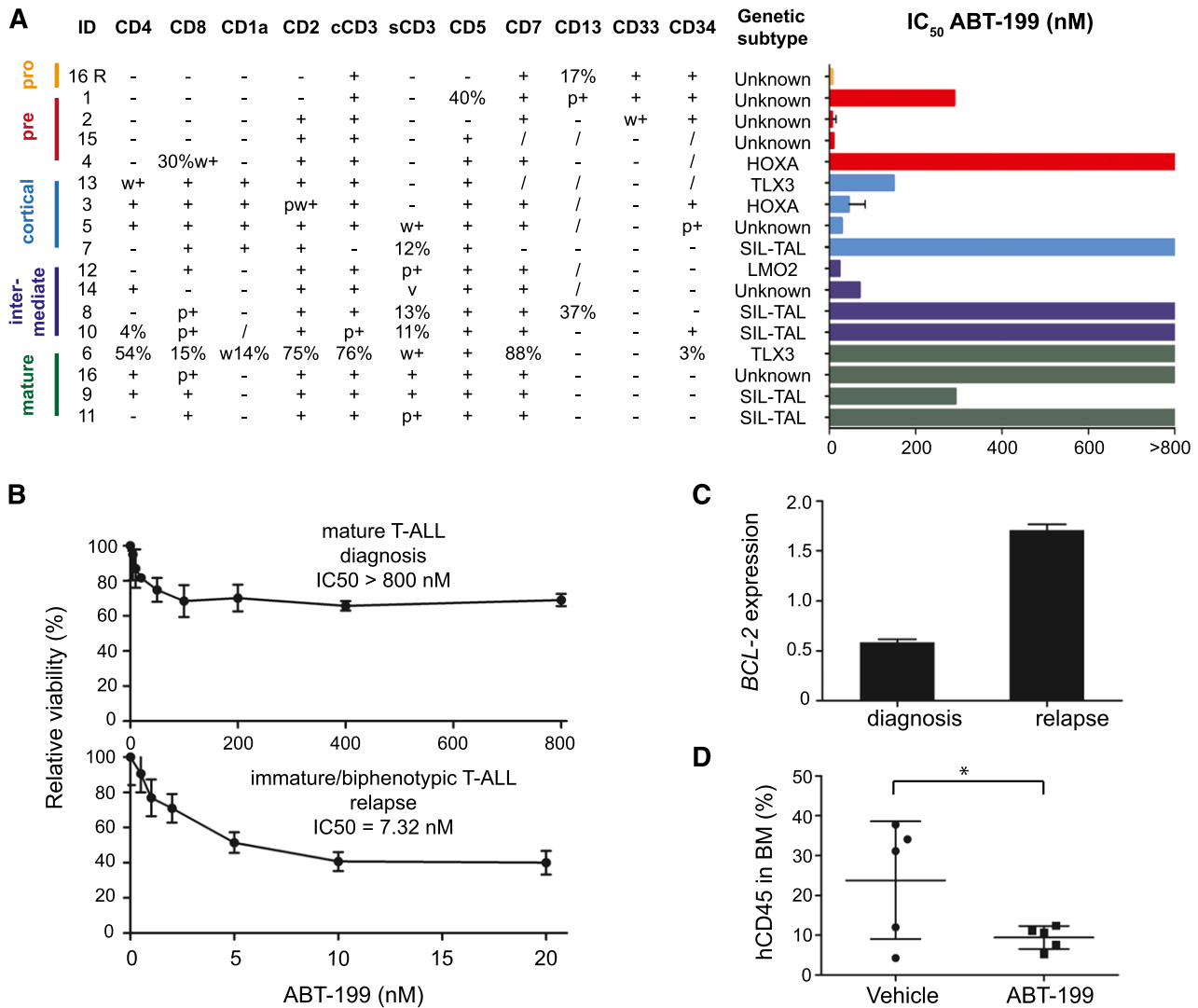


**Figure 5. ABT-199 sensitivity in primary human T-ALL patient samples.** (A) ABT-199 IC<sub>50</sub> values for a panel of primary T-ALL samples. Patient samples are classified based on their immunophenotype in pro-, pre-, cortical, intermediate between cortical, and mature T-ALL with markers scored on the blast gate. Molecular classification is based on fluorescence in situ hybridization and/or expression analysis. (B) Cell viability of diagnostic and relapse material from T-ALL patient 16 after 16 hours of ABT-199 treatment using different concentrations relative to cells incubated with dimethylsulfoxide (100%). (C) *BCL-2* expression (quantitative real-time polymerase chain reactions, calibrated normalized relative quantities values and corresponding standard errors) analysis of diagnostic and relapse material obtained from T-ALL patient 16. The expression was standardized against *B2M*, *HPRT1*, *RPL13A*, and *TBP*. (D) Percentage of human CD45 in the bone marrow of NSG mice injected with a patient-derived xenograft from T-ALL #3 (MLL rearranged, HOXA-positive) after 7 days of treatment with vehicle or ABT-199. /, not known; BM, bone marrow; cCD3, cytoplasmic CD3; p+, partial positive; R, relapse; s, surface; v, variable; w, weak. \**P* = .0498.

thymic precursors will undergo the process of  $\beta$ -selection, which coincides with loss of *BCL-2* expression as the cells move into the  $\alpha\beta$  lineage. Hence, we observed the lowest levels of *BCL-2* in CD3<sup>-</sup>CD4<sup>+</sup>CD8<sup>+</sup> T-cells. In contrast, *BCL-2L1* showed an opposite pattern of expression with high *BCL-2L1* levels in CD4<sup>+</sup>CD8<sup>+</sup> T-cells, suggesting an antiapoptotic switch from *BCL-2* to *BCL-2L1* during human T-cell maturation. Finally, CD28<sup>-</sup>CD4<sup>+</sup> ISP cells that rearrange their TCR- $\Delta$  and TCR- $\beta$  into functional TCR $\delta$  and TCR $\beta$  chains will develop into the  $\gamma\delta$  lineage, and these were shown to retain most of their *BCL-2* expression. Altogether, *BCL-2* expression analysis in 2 genetically well-defined primary T-ALL patient cohorts and sorted subsets of T-cells confirmed the tight association between normal and malignant T-cell development, and provided a rationale for targeting *BCL-2* in immature subtypes of human T-ALL.

In vitro analysis of human T-ALL cell lines showed marked differences between cell lines that reflect different molecular genetic

T-ALL subtypes and unraveled a significant association between ABT-199 sensitivity and *BCL-2* expression levels. Most notably, the T-ALL cell line LOUCY showed the highest *BCL-2* expression and was highly sensitive to *BCL-2* inhibition by ABT-199 both in vitro<sup>24</sup> and in vivo using xenografts of human LOUCY cells. Although the gene expression profile of the T-ALL cell line LOUCY closely resembles the gene signature observed in lymphoblasts from primary immature human T-ALLs,<sup>25</sup> this cell line shows characteristic activation of *HOXA* expression due to the presence of the *SET-NUP214* fusion oncogene,<sup>35</sup> which has been associated with corticosteroid and chemotherapy resistance.<sup>36</sup> In addition, the LOUCY cell line is TCR $\gamma\delta$ -positive, suggesting that it combines immature transcriptional features with a mature TCR $\gamma\delta$  immunophenotype. Therefore, its high *BCL-2* expression mimics normal T-cell development where *BCL-2* levels remain high in T-cells that differentiate along the  $\gamma\delta$  lineage. Altogether, these data suggest that *BCL-2* levels could

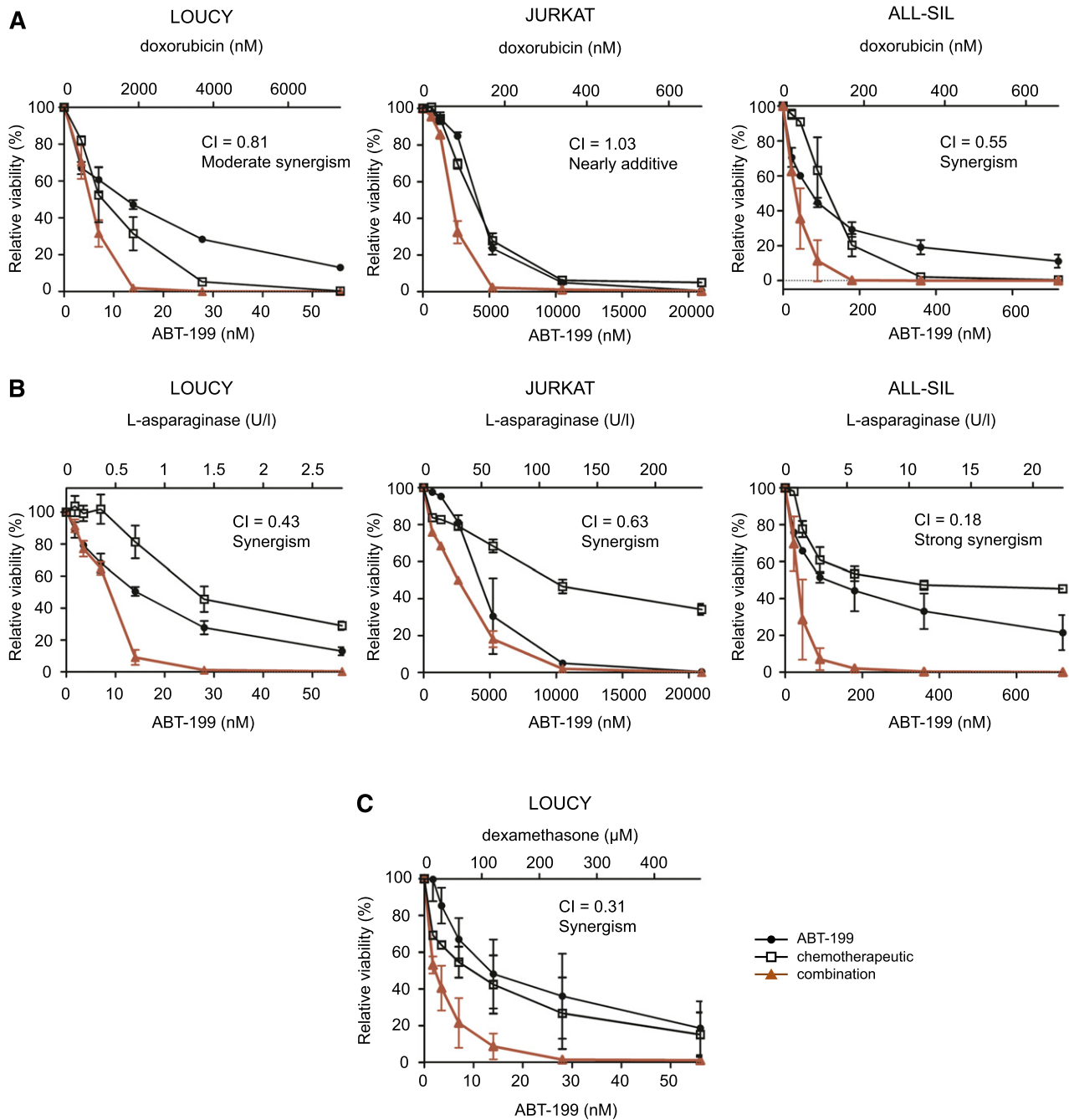


**Figure 6. ABT-199 in combination with chemotherapeutic agents in human T-ALL cell lines.** The effect of monotherapy or combination therapy on the viability of T-ALL cell lines is visualized. Cell viability is expressed relative to cells treated with dimethylsulfoxide and the average and standard deviation of 2 independent experiments is plotted for each combination. Combination of ABT-199 with doxorubicin (A) or L-asparaginase (B) in the T-ALL cell lines LOUCY, JURKAT, and ALL-SIL. (C) Combination of ABT-199 and dexamethasone is only shown for the LOUCY cell line. The combination index (CI) shown represents the average of the CIs at the ED50, ED75, and ED90 effect levels for each experiment.  $0.9 < CI < 1.1$ : nearly additive;  $0.85 < CI < 0.9$ : slight synergism;  $0.7 < CI < 0.85$ : moderate synergism;  $0.3 < CI < 0.7$ : synergism;  $0.1 < CI < 0.3$ : strong synergism;  $CI < 0.1$ : very strong synergism.

predict ABT-199 sensitivity in human T-ALL and suggest that BCL-2 inhibition might be particularly relevant as a novel therapeutic strategy in immature and *HOXA*-positive T-ALL.

To obtain further evidence for the close association between tumor immune phenotype, BCL-2 expression, and ABT-199 sensitivity, we used the Lck-Lmo2 transgenic mouse model (K.R. and T.H.R., manuscript in preparation). The Lck-Lmo2 transgenic shows similar characteristics as the CD2-Lmo2 mouse model,<sup>11,26</sup> in which *Lmo2* promotes self-renewal of preleukemic thymocytes and sets the

stage for the accumulation of additional genetic mutations required for leukemic transformation.<sup>37</sup> In this model, *BCL-2* expression was associated with the differentiation arrest of the tumor cells and defined the ABT-199 response of these murine tumors. Therefore, the tumor susceptibility toward BCL-2 inhibition is initially dictated by the tumor cell of origin and is conserved in mice.

In a next step, ABT-199 was able to affect the viability of primary T-ALL samples in vitro. Especially CD4<sup>+</sup>CD8<sup>-</sup> samples and samples belonging to the pro-T, pre-T, and cortical T immunophenotypic



maturation stages were responsive to ABT-199 treatment, whereas mature subtypes that differentiate along the  $\alpha\beta$  lineage were largely insensitive. Intriguingly, a T-ALL patient that was characterized by an immunophenotypic switch between diagnosis and relapse further exemplified the association between ABT-199 sensitivity and tumor immunophenotype. Notably, immature therapy-resistant leukemia cells at relapse were highly sensitive to ABT-199 in vitro, suggesting that BCL-2 inhibition could also serve as a promising therapeutic strategy for refractory T-cell leukemias. In addition, and as previously shown,<sup>38</sup> in vitro sensitivity of an *MLL* rearranged T-ALL patient corresponded with reduced tumor burden upon ABT-199 treatment in vivo using a patient-derived xenograft with material from that *HOXA*-positive T-ALL. Based on these observations, we hypothesize that immunophenotypic features and *BCL-2* expression levels largely determine ABT-199 sensitivity in human T-ALL. Importantly, our study confirms the recent work from Chonghaile et al,<sup>39</sup> which was mainly focused on the potential use of ABT-199 for the treatment of human ETP-ALL. However, our study suggests that genetic subtypes of human T-ALL that may benefit from ABT-199 treatment may extend beyond ETP-ALL and could also include *TLX1*, *TLX3*, or *HOXA*-positive T-ALLs, as well as mature TCR $\gamma\delta$ -positive leukemias.

Most conventional chemotherapeutic agents execute their action via the mitochondrial pathway of apoptosis by activation of proapoptotic or inactivation of antiapoptotic BCL-2 family proteins. Whether malignant cells are sensitive to a chemotherapeutic agent may depend on their pretreatment priming (ie, the proximity of a malignant cell to an apoptotic threshold).<sup>40</sup> Given this, the combination of ABT-199 and chemotherapeutic agents could increase the chemosensitivity of malignant cells by reduction of their antiapoptotic reserve.<sup>40</sup> Moreover, the combination of ABT-199 with chemotherapeutic agents or other targeted therapies could avoid the emergence of therapy resistance and result in reduced cytotoxic side effects due to lower chemotherapy dosage. In myeloid and ALL cell lines, ABT-737 was shown to increase sensitivity toward chemotherapeutic agents.<sup>40,41</sup> In addition, a strong synergism between ABT-199 and cytarabine has been previously reported in the T-ALL cell line LOUCY.<sup>24</sup> These findings were further extended in our study, in which we showed synergistic effects between ABT-199, doxorubicin, L-asparaginase, and dexamethasone mainly in T-ALL cell lines with low ABT-199 IC<sub>50</sub> values.

Altogether, our study defines BCL-2 as an attractive molecular target in human T-ALL and provides a rationale for including T-ALL patients in clinical trials for the BH3-mimetic ABT-199 in combination with conventional chemotherapeutics.

## Acknowledgments

The authors thank Béatrice Lintermans and Lindy Reunes for excellent technical assistance, the in vivo small animal imaging laboratory (Innovative Flemish in vivo imaging technology, [INFINITY]) at Ghent University Hospital, and Wim Schuermans for interpretation of immunophenotypic patient data.

This work was supported by the Research Foundation Flanders (FWO) research projects G.0202.09, G.0869.10N (F.S.), G065614, 3GA00113N, and G.0C47.13N (P.V.V.); G0B2913N and 3G002711 (T.T.), PhD grant (S.P.), postdoctoral grants (T.T., P.V.V., S.G., and I.V.d.W.) and a senior clinical investigator grant (B.P.); the Belgian Foundation against Cancer (F.S. and S.G.) and grant 2010-187 (T.L.); the Flemish Liga against Cancer (VLK) Postdoc grant (F.M.); Ghent University (Concerted Research Action grant 12051203) (F.S.); the Cancer Plan from the Federal Public Service of Health (F.S., Y.B.), the Children Cancer Fund Ghent (F.S., Y.B.); the Belgian Program of Interuniversity Poles of Attraction (36509110) (F.S.); additional funding by the Cancéropole Ile-De-France, the Cartes d'Identité des Tumeurs program from the Ligue Contre le Cancer, European Research Council Consolidator Grant 311660, the Saint-Louis Institute program (ANR-10-IBHU-0002 to J.S.); and grants from Leukaemia & Lymphoma Research, Medical Research Council, and the Wellcome Trust (LMo2 mouse model work to T.H.R.).

## Authorship

Contribution: S.P. analyzed experiments; S.P., F.M., S.G., I.V.d.W., C.E.d.B., and S.D. performed experiments; D.B., E.C., and J.S. provided RNA of primary T-ALL patient samples for gene expression analysis; T.L., B.D.M., and Y.B. provided primary T-ALL patient samples; K.R. and T.H.R. shared cells of the Lck-LMo2 mouse model; J.C., B.P., F.S., and P.V.V. designed experiments, directed research, and analyzed data; S.P., J.C., B.P., F.S., and P.V.V. wrote the paper; and all authors read and edited the manuscript.

Conflict-of-interest disclosure: The authors declare no competing financial interests.

Correspondence: Pieter Van Vlierberghe, Center for Medical Genetics Ghent, Ghent University Hospital, Medical Research Building, Room 120.032, De Pintelaan 185, 9000 Ghent, Belgium; e-mail: pieter.vanvlierberghe@ugent.be.

## References

- Barrett AJ, Horowitz MM, Pollock BH, et al. Bone marrow transplants from HLA-identical siblings as compared with chemotherapy for children with acute lymphoblastic leukemia in a second remission. *N Engl J Med*. 1994;331(19):1253-1258.
- Goldberg JM, Silverman LB, Levy DE, et al. Childhood T-cell acute lymphoblastic leukemia: the Dana-Farber Cancer Institute acute lymphoblastic leukemia consortium experience. *J Clin Oncol*. 2003;21(19):3616-3622.
- Van Vlierberghe P, Ferrando A. The molecular basis of T cell acute lymphoblastic leukemia. *J Clin Invest*. 2012;122(10):3398-3406.
- Ferrando AA, Neuberg DS, Staunton J, et al. Gene expression signatures define novel oncogenic pathways in T cell acute lymphoblastic leukemia. *Cancer Cell*. 2002;1(1):75-87.
- Homminga I, Pieters R, Langerak AW, et al. Integrated transcript and genome analyses reveal NKX2-1 and MEF2C as potential oncogenes in T cell acute lymphoblastic leukemia. *Cancer Cell*. 2011;19(4):484-497.
- Soulier J, Clappier E, Cayuela JM, et al. HOXA genes are included in genetic and biologic networks defining human acute T-cell leukemia (T-ALL). *Blood*. 2005;106(1):274-286.
- Coustan-Smith E, Mullighan CG, Onciu M, et al. Early T-cell precursor leukaemia: a subtype of very high-risk acute lymphoblastic leukaemia. *Lancet Oncol*. 2009;10(2):147-156.
- Zuurbier L, Gutierrez A, Mullighan CG, et al. Immature MEF2C-dysregulated T-cell leukemia patients have an early T-cell precursor acute lymphoblastic leukemia gene signature and typically have non-rearranged T-cell receptors. *Haematologica*. 2014;99(1):94-102.
- Inukai T, Kiyokawa N, Campana D, et al. Clinical significance of early T-cell precursor acute lymphoblastic leukaemia: results of the Tokyo Children's Cancer Study Group Study L99-15. *Br J Haematol*. 2012;156(3):358-365.
- Van Vlierberghe P, Ambesi-Impombato A, De Keersmaecker K, et al. Prognostic relevance of integrated genetic profiling in adult T-cell acute lymphoblastic leukemia. *Blood*. 2013;122(1):74-82.
- Larson RC, Osada H, Larson TA, Lavenir I, Rabbitts TH. The oncogenic LIM protein Rbtrn2 causes thymic developmental aberrations that precede malignancy in transgenic mice. *Oncogene*. 1995;11(5):853-862.
- Bene MC, Castoldi G, Knapp W, et al; European Group for the Immunological Characterization of Leukemias (EGIL). Proposals for the

- immunological classification of acute leukemias. *Leukemia*. 1995;9(10):1783-1786.
13. Souers AJ, Levenson JD, Boghaert ER, et al. ABT-199, a potent and selective BCL-2 inhibitor, achieves antitumor activity while sparing platelets. *Nat Med*. 2013;19(2):202-208.
  14. Niu X, Wang G, Wang Y, et al. Acute myeloid leukemia cells harboring MLL fusion genes or with the acute promyelocytic leukemia phenotype are sensitive to the Bcl-2-selective inhibitor ABT-199. *Leukemia*. 2014;28(7):1557-1560.
  15. Pan R, Hogdal LJ, Benito JM, et al. Selective BCL-2 inhibition by ABT-199 causes on-target cell death in acute myeloid leukemia. *Cancer Discov*. 2014;4(3):362-375.
  16. Vogler M, Dinsdale D, Dyer MJ, Cohen GM. ABT-199 selectively inhibits BCL2 but not BCL2L1 and efficiently induces apoptosis of chronic lymphocytic leukaemic cells but not platelets. *Br J Haematol*. 2013;163(1):139-142.
  17. Touzeau C, Dousset C, Le Gouill S, et al. The Bcl-2 specific BH3 mimetic ABT-199: a promising targeted therapy for t(11;14) multiple myeloma. *Leukemia*. 2014;28(1):210-212.
  18. Vaillant F, Merino D, Lee L, et al. Targeting BCL-2 with the BH3 mimetic ABT-199 in estrogen receptor-positive breast cancer. *Cancer Cell*. 2013;24(1):120-129.
  19. Vandenberg CJ, Cory S. ABT-199, a new Bcl-2-specific BH3 mimetic, has in vivo efficacy against aggressive Myc-driven mouse lymphomas without provoking thrombocytopenia. *Blood*. 2013;121(12):2285-2288.
  20. BCL-2 inhibitor yields high response in CLL and SLL. BCL-2 inhibitor yields high response in CLL and SLL. *Cancer Discov*. 2014;4(2):OF5.
  21. Clappier E, Gerby B, Sigaux F, et al. Clonal selection in xenografted human T cell acute lymphoblastic leukemia recapitulates gain of malignancy at relapse. *J Exp Med*. 2011;208(4):653-661.
  22. Reich M, Liefeld T, Gould J, Lerner J, Tamayo P, Mesirov JP. GenePattern 2.0. *Nat Genet*. 2006;38(5):500-501.
  23. Taghon T, Waegemans E, Van de Walle I. Notch signaling during human T cell development. *Curr Top Microbiol Immunol*. 2012;360:75-97.
  24. Anderson NM, Harrold I, Mansour MR, et al. BCL2-specific inhibitor ABT-199 synergizes strongly with cytarabine against the early immature LOUCY cell line but not more-differentiated T-ALL cell lines. *Leukemia*. 2014;28(5):1145-1148.
  25. Van Vlierberghe P, Ambesi-Impiombato A, Perez-Garcia A, et al. ETV6 mutations in early immature human T cell leukemias. *J Exp Med*. 2011;208(13):2571-2579.
  26. Larson RC, Fisch P, Larson TA, et al. T cell tumours of disparate phenotype in mice transgenic for Rbnt-2. *Oncogene*. 1994;9(12):3675-3681.
  27. Pui CH, Robison LL, Look AT. Acute lymphoblastic leukaemia. *Lancet*. 2008;371(9617):1030-1043.
  28. Hanahan D, Weinberg RA. The hallmarks of cancer. *Cell*. 2000;100(1):57-70.
  29. Adams JM, Cory S. The Bcl-2 apoptotic switch in cancer development and therapy. *Oncogene*. 2007;26(9):1324-1337.
  30. Juin P, Geneste O, Gautier F, Depil S, Campone M. Decoding and unlocking the BCL-2 dependency of cancer cells. *Nat Rev Cancer*. 2013;13(7):455-465.
  31. Oltsdorf T, Elmore SW, Shoemaker AR, et al. An inhibitor of Bcl-2 family proteins induces regression of solid tumours. *Nature*. 2005;435(7042):677-681.
  32. Tse C, Shoemaker AR, Adickes J, et al. ABT-263: a potent and orally bioavailable Bcl-2 family inhibitor. *Cancer Res*. 2008;68(9):3421-3428.
  33. Roberts AW, Seymour JF, Brown JR, et al. Substantial susceptibility of chronic lymphocytic leukemia to BCL2 inhibition: results of a phase I study of navitoclax in patients with relapsed or refractory disease. *J Clin Oncol*. 2012;30(5):488-496.
  34. Zhang H, Nimmer PM, Tahir SK, et al. Bcl-2 family proteins are essential for platelet survival. *Cell Death Differ*. 2007;14(5):943-951.
  35. Van Vlierberghe P, van Grotel M, Tchinda J, et al. The recurrent SET-NUP214 fusion as a new HOXA activation mechanism in pediatric T-cell acute lymphoblastic leukemia. *Blood*. 2008;111(9):4668-4680.
  36. Ben Abdelali R, Roggy A, Leguay T, et al. SET-NUP214 is a recurrent  $\gamma\delta$  lineage-specific fusion transcript associated with corticosteroid/chemotherapy resistance in adult T-ALL. *Blood*. 2014;123(12):1860-1863.
  37. McCormack MP, Young LF, Vasudevan S, et al. The Lmo2 oncogene initiates leukemia in mice by inducing thymocyte self-renewal. *Science*. 2010;327(5967):879-883.
  38. Suryani S, Carol H, Chonghaile TN, et al. Cell and molecular determinants of in vivo efficacy of the BH3 mimetic ABT-263 against pediatric acute lymphoblastic leukemia xenografts. *Clin Cancer Res*. 2014;20(17):4520-4531.
  39. Chonghaile TN, Roderick JE, Glenfield C, et al. Maturation stage of T-cell acute lymphoblastic leukemia determines BCL-2 versus BCL-XL dependence and sensitivity to ABT-199. *Cancer Discov*. 2014;4(9):1074-1087.
  40. Ni Chonghaile T, Sarosiek KA, Vo TT, et al. Pretreatment mitochondrial priming correlates with clinical response to cytotoxic chemotherapy. *Science*. 2011;334(6059):1129-1133.
  41. Kang MH, Kang YH, Szymanska B, et al. Activity of vincristine, L-ASP, and dexamethasone against acute lymphoblastic leukemia is enhanced by the BH3-mimetic ABT-737 in vitro and in vivo. *Blood*. 2007;110(6):2057-2066.